Infrared Spectra and Molecular Relaxation Dynamics of LiSCN in Polyethers: Toward the Polymer−Electrolyte

Rebecca Kreitner,[†] Jessie Park,[†] Meizhen Xu,[†] Edward M. Eyring,[‡] and Sergio Petrucci*[,†]

Weber Research Institute, Polytechnic University, Route 110, Farmingdale, New York 11735, and Department of Chemistry, University of Utah, Salt Lake City, Utah 84112

Received December 5, 1995; Revised Manuscript Received April 25, 1996[⊗]

ABSTRACT: Infrared spectra of the antisymmetric stretching mode ("CN stretch") of the SCN^- anion for LiSCN dissolved in the ethers 1,2-dimethoxyethane (1,2-DME), diglyme, triglyme, and poly(ethylene oxide) dimethyl ether of average molar mass 250 (PEO-250) at various concentrations at 25 °C reveal that the electrolyte LiSCN is heavily associated to form contact ion pairs LiNCS. A minor amount exists as solvent-separated and/or free ions (Li^+S, ^-NCS or ^-NCS), the so-called "spectroscopically free" thiocyanate ions. The molecular dynamics of the same electrolyte in the same ethers have been studied by ultrasonic (except for triglyme because of limited solubility of LiSCN) and microwave dielectric relaxation techniques. The ultrasonic relaxation spectra, in the frequency range 1−400 MHz, can be interpreted by the sum of two Debye relaxation processes, which are taken to reflect the multistep Eigen process: $Li^+S_y + {}^-NCS \underset{1}{\rightleftharpoons} Li^+O_x$, $^-NCS \underset{2}{\rightleftharpoons} Li^+O_{x-1}$, $^-NCS \underset{3}{\rightleftharpoons} LiNCS$. Here S is a solvent molecule, whereas O denotes a binding post of the solvent such as an oxygen atom. The fast observed process is attributed to step 2, coupled to the faster step 1, through a pre-equilibration constant K_1. The "slow" observed process is interpreted as due to step 3, coupled with the two faster processes 1 and 2. The interesting finding is that, whereas for 1,2-DME the data follow a separate trend, the data for diglyme and for PEO-250 appear to have the same concentration dependence of both the relaxation times τ_I and τ_{II}. Yet, the repetition unit $(-CH_2CH_2O-)_n$ number n is 2 for diglyme and 4.6 for PEO-250. For τ_{II} *vs* c_{LiSCN}, the common concentration dependencies extend to the data in PEO-400. These results are interpreted as meaning that the observed processes, characterized by τ_I and τ_{II}, reflect the local relaxation dynamics of desolvation of ions by interchange of the $-CH_2CH_2O-$ groups by ^-NCS, *independent of the increase of the chain length of the polyether, within the above range of n values.* The UHF-microwave dielectric relaxation spectra of LiSCN in the above solvent systems 1,2-DME, diglyme, and PEO-250 at 25 °C and at a concentration $C \simeq 0.1$ mol dm^{-3}, when coupled with the results of the same spectra for triglyme, *reveal a correlation between the solute dielectric relaxation time $\tau_I(D)$ and the repetition number n of the $(-CH_2CH_2O-)$ units of the polyether.* This is taken to indicate that the rotational relaxation time of the solute LiNCS dipoles depends on the chain length of the polyether; namely, $\tau_I(D)$ reflects the long-range dynamics of the solvent.

Introduction

The ionic association and molecular dynamics of lithium salts in simple ethers, such as THF and 1,2-DME, have been studied previously in our laboratories.[1] We have also investigated[2] lithium salts dissolved in polyethers, which are potential polymer−electrolyte systems for solid-state batteries. There are well-established theories of transport of ions in simple liquids such as the Fuoss−Onsager continuum theory for dilute solutions[3] and the mean spherical approximation (MSA) theory, which has recently been extended[4] to ∼1 mol dm^{-3}.

For polymer−electrolyte systems, the so-called percolation theory[5] and its predecessor, the free volume theory,[6] have been proposed, with the basic idea that, in order for ions to move, the polymer chains must rearrange themselves with their own "rejuvenation time".[5] There is no conceptual transition between the continuum theories[3,4] and the percolation[5] and free volume[6] theories, mostly because of a lack of systematic experimental studies covering the gap between the two fields.

In order to offer the electrochemist experimental results amenable to realistic modeling for future theories, we reasoned that data obtained by various experimental methods were required for lithium salts dissolved in solvents ranging from the simplest polyether, such as 1,2-DME, to the polymeric polyethers such as PEO-250 and, in some instances, PEO-400. In other words, the repeat unit $(-CH_2CH_2O-)_n$ needed to be extended from $n = 1$ as in 1,2-DME, to $n = 4.6$ in PEO-250, and to $n = 8.0$ in PEO-400.

With this in mind, we have produced infrared spectra, ultrasonic relaxation spectra, and dielectric relaxation spectra of some of the above systems, using LiSCN as a model electrolyte. For clarity of presentation, the results and calculations for the three methods used will be given separately below.

Experimental Section

The instrumentation and experimental procedures for infrared, ultrasonic, and microwave spectrometries have been described before.[2] As for the materials, LiSCN hydrate (Aldrich) was dried in vacuo, first at room temperature and, after 1 day, at increasing temperatures up to 110 °C and constancy of weight. 1,2-DME (Fluka) was refluxed over benzophenone until a blue coloration appeared, and then it was distilled at ∼10 Torr of pressure. Diglyme, triglyme, and PEO-250 were Fluka products and were dried over molecular sieves.

Results and Calculations

(a) Infrared Spectra. Figures 1A, 1C, 1E, and 1G show the infrared envelope, expressed in absorbance A *vs* the wavenumber $\bar{\nu}$, for a representative spectrum of

[†] Polytechnic University.
[‡] University of Utah.
[⊗] Abstract published in *Advance ACS Abstracts,* June 1, 1996.

S0024-9297(95)01791-8 CCC: $12.00

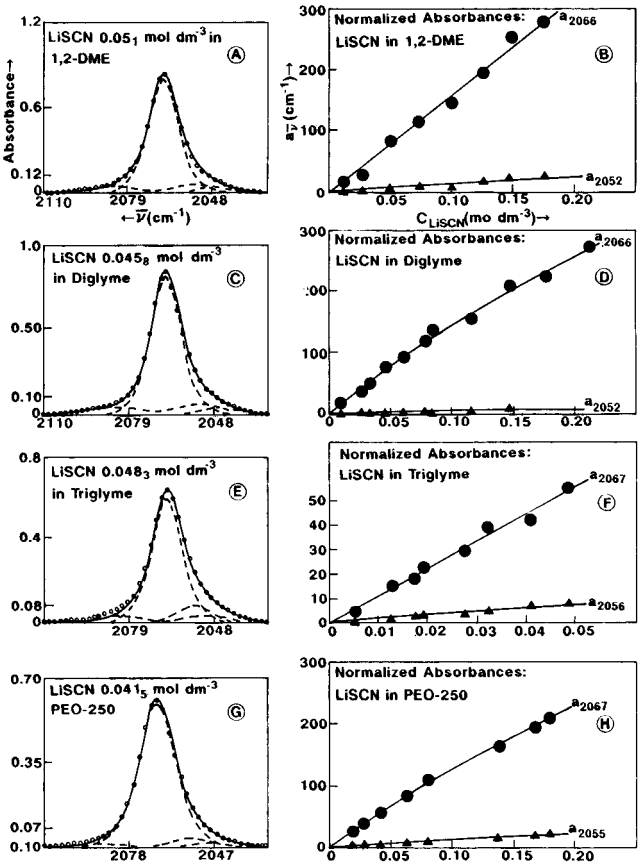

Figure 1. (A,C,E,G) Representative digitized infrared spectra of the "CN stretch" region of LiSCN in the solvents 1,2-DME, diglyme, triglyme, and PEO-250 at 25 °C. (B,D,F,H) Normalized maximum absorbances $a_{\bar{\nu}} = (A_{\bar{\nu}}°/l)$ per unit cell length *vs* concentration of electrolyte for LiSCN in the solvents 1,2-DME, diglyme, triglyme, and PEO-250 at 25 °C.

the SCN^- anion in the 2100−2000 cm^{-1} region ("CN stretch") for the systems LiSCN in 1,2-DME, diglyme, triglyme, and poly(ethylene oxide) of average molar mass 250 (PEO-250) at 25 °C.

The solid lines in Figures 1A, 1C, 1E, and 1G correspond to the sum of two Gaussian−Lorentzian bands for the solutes centered around 2066 and 2048−2056 cm^{-1}, respectively. Where necessary, small bands for the solvents have been added (dashed lines and dashed areas in the above figures). The solvents alone have been previously studied in the same wavenumber ranges.

All the Gaussian−Lorentzian bands (dashed lines) correspond to the product functions:[7]

$$A_{\bar{\nu}} = A_{\bar{\nu}}° \exp\left(-\frac{(\bar{\nu}-\bar{\nu}_0)^2}{2\sigma^2}\right)\left(1+\frac{(\bar{\nu}-\bar{\nu}_0)^2}{\sigma^2}\right)^{-1} \qquad (1)$$

where $A_{\nu}°$ is the absorbance maximum of the band centered at $\bar{\nu}_0$, σ^2 is the variance, with the standard error $\sigma = (\Delta\bar{\nu})_{1/2}/1.46$, and $(\Delta\bar{\nu})_{1/2}$ is the width of the band at half-maximum absorbance given by $A_0/2$.

Table 1 reports the parameters of the bands $A_{\bar{\nu}}°$, $\bar{\nu}_0$, and $\Delta\bar{\nu}_{1/2}$, used to fit the spectral envelopes for the various systems investigated, together with the sample cell lengths l.

Figures 1B, 1D, 1F, and 1H report the normalized maximum absorbance per unit cell length $a_{\bar{\nu}} = A_{\bar{\nu}}°/l$ plotted *vs* the electrolyte concentration C_{LiSCN}. The solid lines of the above figures are the functions $a_{\bar{\nu}} = \alpha_{\bar{\nu}} + \beta_{\bar{\nu}}C_{LiSCN} + \gamma_{\bar{\nu}}C^2_{LiSCN} + \delta_{\bar{\nu}}C^3_{LiSCN}$, calculated by nonlinear or linear regression (the latter for $\gamma_{\bar{\nu}} = \delta_{\bar{\nu}} = 0$). Table 2 reports the above coefficients $\alpha_{\bar{\nu}}$, $\beta_{\bar{\nu}}$, $\gamma_{\bar{\nu}}$, and $\delta_{\bar{\nu}}$ together with the determination coefficient r^2 (squared correlation coefficients r) used for the fit.

From the relative values of $a_{\bar{\nu}}$ ($\bar{\nu} \cong 2066$ cm^{-1}) compared with $a_{\bar{\nu}}$ ($\bar{\nu} \cong 2050$−2056 cm^{-1}), it appears that the species corresponding to $\bar{\nu} \cong 2066$ cm^{-1} is the predominant species in solution. Normal coordinate

Table 1. Infrared Parameters Related to the "CN Stretch" Envelope of the Thiocyanate Ion and Cell Length l for LiSCN in Polyethers at 25 °C

C_{LiSCN} (mol dm^{-3})	$\bar{\nu}_{2066}$ (cm^{-1})	$A°_{2066}$	$(\Delta\bar{\nu}_{2066})_{1/2}$ (cm^{-1})	$\bar{\nu}_{2050}$ (cm^{-1})	$A°_{2050}$	$(\Delta\bar{\nu}_{2050})_{1/2}$ (cm^{-1})	l (cm)
			Solvent: 1,2-DME				
0.0132	2066.3	0.168	11.4	2052.0	0.015	15.5	0.01057
0.0292	2066.3	0.300	11.4	2052.0	0.032	15.5	0.01058
0.051	2066.3	0.893	11.4	2052.0	0.064	15.5	0.01058
0.0754	2066.7	1.236	11.4	2052.0	0.086	15.5	0.01082
0.102	2066.7	0.738	11.4	2052.0	0.026	15.5	0.00511
0.127	2066.7	0.997	11.4	2052.0	0.077	15.5	0.005105
0.148	2067.2	1.282	11.4	2052.0	0.124	15.5	0.005076
0.176	2067.2	1.412	11.4	2052.0	0.124	15.5	0.005082
			Solvent: Diglyme				
0.0098	2066.6	0.155	13.0	2048.5	0.013	13.0	0.01077
0.0268	2066.0	0.375	13.0	2048.5	0.023	13.0	0.01057
0.0335	2066.0	0.540	13.0	2048.5	0.028	13.0	0.01098
0.0458	2066.3	0.810	12.7	2048.5	0.038	13.0	0.01058
0.0610	2066.3	0.975	12.7	2048.5	0.038	13.0	0.01056
0.0787	2066.7	1.245	12.1	2048.5	0.047	13.0	0.01058
0.0841	2066.4	1.438	12.1	2048.5	0.038	13.0	0.01058
0.116	2066.7	0.781	12.1	2048.5	0.014	13.0	0.0051
0.147	2066.7	1.051	12.1	2048.5	0.028	13.0	0.0051
0.176	2067.0	0.633	12.3	2048.5			0.00285
0.211	2067.2	0.773	12.3	2048.5			0.00282
			Solvent: Triglyme				
0.0052_2	2066.5	0.050	13	2056	0.007	14	0.01060
0.0129	2067	0.159	13	2056	0.021	14	0.01058
0.0175	2067	0.197	13	2056	0.024	14	0.01057
0.0191	2067	0.244	13	2056	0.032	14	0.01058
0.0274	2067	0.312	13	2056	0.032	14	0.0158
0.0323	$2067._2$	0.415	13	2056	0.048	14	0.01058
0.0409	$2067._5$	0.442	13	2056	0.072	14	0.01058
0.0485	$2066._3$	0.589	13	2056	0.078	14	0.01061
			Solvent: PEO-250				
0.0199	2067.3	0.257	14.4	2055.5	0.035	13.5	0.01057
0.0280	2067.0	0.385	14.4	2055.5	0.035	13.5	0.01058
0.0415	2067.0	0.590	14.4	2055.5	0.035	13.5	0.01056
0.0634	2067.3	0.875	14.0	2055.5	0.065	13.5	0.01056
0.0797	2067.3	1.175	13.8	2055.5	0.086	13.5	0.01056
0.138	2067.7	0.819	13.8	2055.5	0.080	13.5	0.00507
0.167	2067.7	0.552	14.0	2055.5	0.057	13.5	0.00288
0.178	2067.7	0.592	14.0	2055.5	0.057	13.5	0.00283

Table 2. Results of the Nonlinear and Linear Regression Analysis for the Normalized Absorbances $a_{\bar{\nu}}$ *vs* C_{LiSCN} for LiSCN in the Solvents 1,2-DME, Diglyme, Triglyme, and PEO-250 at 25 °C[a]

solvent	α_{2066}	β_{2066}	γ_{2066}	δ_{2066}	r^2
1,2-DME	−2.366	1.595×10^3			0.993
diglyme	−0.601	1.763×10^3	-4.092×10^3	8.721×10^3	0.997
triglyme	−0.0055	1.116×10^3			0.993
PEO-250[b]	−0.456	1.504×10^3	-3.077×10^3	6.384×10^3	0.99_8

solvent	α_{2050}	β_{2050}	γ_{2050}	δ_{2050}	r^2
1,2-DME	0.489	131.99			0.908
diglyme	0.391	37.116			0.81
triglyme	−0.057	150.0			0.980
PEO-250[b]	-0.095_5	113.9			0.99_3

[a] In the above, $a_{2066} = \alpha_{2066} + \beta_{2066}C_{LiSCN} + \gamma_{2066}C^2_{LiSCN} + \delta_{2066}C^3_{LiSCN}$ and $a_{2050} = \alpha_{2050} + \beta_{2050}C_{LiSCN}$. [b] For triglyme and PEO-250, the low-absorbance Gaussian−Lorentzian band is centered at $\bar{\nu}° \cong 2056$−2055 cm^{-1} rather than at $\bar{\nu}° \cong 2052$−2048 cm^{-1}.

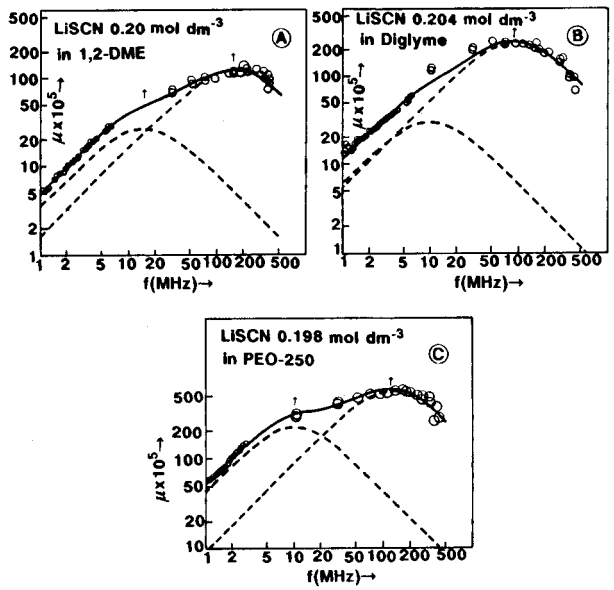

Figure 2. (A−C) Representative ultrasonic relaxation spectra in the form of the excess sound absorption per wavelength, μ, *vs* the frequency f for LiSCN in the solvents 1,2-DME, diglyme, and PEO-250 at 25 °C.

analysis performed[8] for the thiocyanate ion in various solvents for low permittivity ϵ ($\epsilon \leq 10$) assigns the band at $\bar{\nu} \cong 2066$ cm^{-1} to the contact species LiNCS and the band at $\bar{\nu} \cong 2050$ or 2056 cm^{-1} to the spectroscopically free $^{-}$NCS ions (free ions and solvent-separated ion pairs).

Hence, for the above systems, the infrared spectra suggest that the majority of Li^+ exists as contact ion pairs, LiNCS, with only a minor amount existing either as free or as solvent-separated ion pairs. This is an important conclusion from this portion of the work, which is going to be relevant for the interpretation of the molecular dynamics of LiSCN in the polyethers studied by the two methods.

(b) Ultrasonic Relaxation Spectra. Figures 2A, 2B, and 2C are representative ultrasonic relaxation spectra, expressed as the excess sound absorption per wavelength $\mu = \alpha_{exc}\lambda$, plotted *vs* the frequency f for LiSCN dissolved in the three solvents 1,2-DME, diglyme, and PEO-250 at 25 °C. (The low solubility of LiSCN in triglyme, ~0.05 mol dm^{-3}, prevented the extension of the study to this solvent.) In the above, $\mu = \alpha_{exc}\lambda = (\alpha - Bf^2)u/f$, where α is the sound absorption coefficient, $\lambda = u/f$ is the wavelength, with u the sound velocity, and $B = (\alpha/f^2)_{f \gg f_I, f_{II}}$ is the ratio α/f^2 at frequencies f much larger than the relaxation frequencies f_I and f_{II}. The latter frequencies correspond to the two Debye functions, components of μ

$$\mu = 2\mu_I \frac{f/f_I}{1 + (f/f_I)^2} + 2\mu_{II} \frac{f/f_{II}}{1 + (f/f_{II})^2} \qquad (2)$$

which have been used to describe the spectral envelopes (solid lines in Figures 2A, 2B, and 2C). μ_I and μ_{II} are the maximum excess sound absorptions per wavelength centered at the two relaxation frequencies f_I and f_{II}. Table 3 reports the values of μ_I, μ_{II}, f_I, and f_{II} and the values of B used to fit the spectra to function (2). u is the sound velocity measured at 10−70 MHz for the various systems in this work.

Figures 3A and 3B report the inverse relaxation times τ_I^{-1} ($=2\pi f_I$) and τ_{II}^{-1} ($=2\pi f_{II}$) for the two processes of eq 2 plotted *vs* C_{LiSCN} for the various systems studied. The plots show individual behavior for the 1,2-DME solution where n in the repeat unit of ($-CH_2CH_2O-$) is equal to one. However, for diglyme ($n = 2$) and PEO-250 ($n = 4.6$), the behavior of τ_I^{-1} and of τ_{II}^{-1} *vs* C_{LiSCN} is the same within experimental error (Figures 3A and 3B). One also notes that the τ_I^{-1} and τ_{II}^{-1} *vs* C_{LiSCN} plots tend to a horizontal line, a behavior already noted before for $LiClO_4$ in polyethers.[9]

As done previously, we propose that the above-observed relaxation processes 1 and 2 are described by the multistep Eigen−Tamm[10] scheme:

Table 3. Ultrasonic Parameters and Sound Velocities u for LiSCN in the Solvent[5] 1,2-DME, Diglyme, and PEO-250 at 25 °C

C_{LiSCN}	$\mu_I \times 10^5$	f_I (MHz)	$\mu_{II} \times 10^5$	f_{II} (MHz)	$B \times 10^{17}$ (cm^{-1} s^2)	$u \times 10^5$ (cm s^{-1})
			Solvent: 1,2-DME			
0.108	60	70	9	10	32.3	1.186
0.154	80	100	18	15	34	1.199
0.20	120	150	27	15	34	1.197
0.30	180	150	40	15	40	1.201
			Solvent: Diglyme			
0.10	130	60	12	8	38	1.295
0.204	240	90	30	10	39	1.308
0.30	350	120	50	9	42	1.307
0.40	380	100	90	10	49	1.327
0.51	500	120	120	9	49	1.331
			Solvent: PEO-250			
0.0736	220	80	60	5	87	1.429
0.108	300	90	120	7	90	1.441
0.147	400	100	170	9	90	1.440
0.198	550	120	220	10	92	1.446

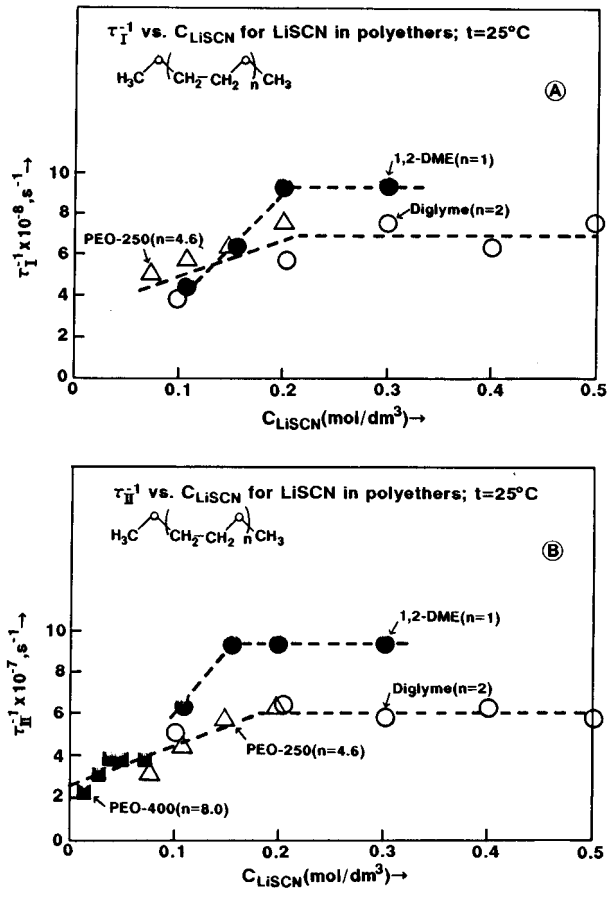

Figure 3. (A,B) Inverse of the relaxation times τ_I^{-1} and τ_{II}^{-1} *vs* C_{LiSCN} for LiSCN in the solvents 1,2-DME, diglyme, and PEO-250 and, for τ_{II}^{-1} *vs* C_{LiSCN}, for LiSCN in PEO-400 at 25 °C.

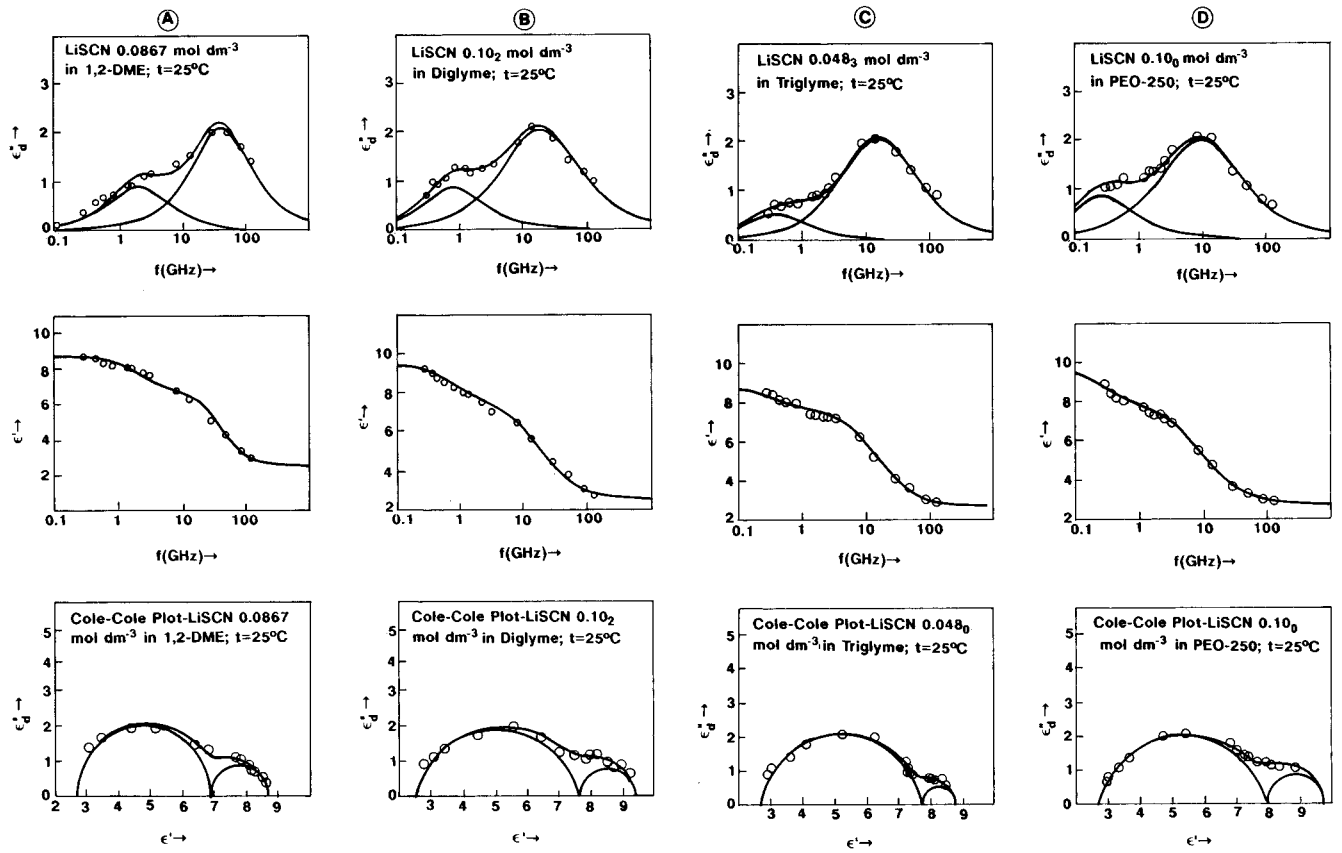

Figure 4. (A–D) Plots of ϵ_d'' and ϵ' *vs* f and Cole–Cole plots of ϵ_d'' *vs* ϵ' for LiSCN solutions in the solvents 1,2-DME, diglyme, triglyme, and PEO-250 at 25 °C. In the above, $\epsilon_d'' = \epsilon'' - \epsilon_\sigma''$, where ϵ_σ'' is the conductance contribution to the loss $\epsilon_\sigma'' = 1.8 \times 10^{12}\sigma/f$, with σ the specific conductivity (S cm^{-1}).

$$Li^+S_y + {}^-NCS \underset{1}{\rightleftharpoons} Li^+O_x, {}^-NCS \underset{2}{\rightleftharpoons} Li^+O_{x-1}, {}^-NCS \underset{3}{\rightleftharpoons} LiNCS \quad (3)$$

Step 1 is a diffusion-controlled process giving rise to a solvent-separated species Li^+O_x,$^-$NCS, with O denoting a binding post of the solvent (such as an oxygen atom of the ($-OCH_2CH_2-$) moiety. Step 2 is a desolvation phenomenon with the formation of a Li^+O_{x-1},$^-$NCS intermediate, which eventually forms the contact species LiNCS. According to the Eigen–Tamm theory,[10] the observed ultrasonic process 1 may correspond to step 2 coupled with the faster step 1. The inverse of the relaxation time τ_I^{-1} for the "fast" process is then given by the equation

$$\tau_I^{-1} = k_2\frac{\theta}{\theta + K_{-1}} + k_{-2} = k_2\Phi + k_{-2} \quad (4)$$

with k_2 and k_{-2} the rate constants for the second step of scheme (3) and K_{-1} representing the inverse of the equilibrium constant $K_1 = k_1/k_{-1}$ for step 1. Also $\theta = 2\sigma C_{LiSCN}$, with σ the degree of dissociation of the ion pair LiNCS.

At high concentration, for $\theta > K_{-1}$, it may occur that $\Phi \cong 1$ and $\tau_I^{-1} \simeq k_2 + k_{-2}$. τ_I^{-1} then becomes independent of concentration as observed (Figure 3A). Similarly, the "slow" process corresponds to step 3 of the Eigen–Tamm scheme (3), coupled with the faster steps 1 and 2. The inverse of the relaxation time τ_{II}^{-1} is given by[10]

$$\tau_{II}^{-1} = k_3\frac{\Phi}{\Phi + K_{-2}} + k_{-3} \quad (5)$$

where $K_{-2} = k_{-2}/k_2$. At high concentration, it may seem that $\Phi > K_{-2}$, and $\tau_{II}^{-1} \simeq k_3 + k_{-3}$; namely, τ_{II}^{-1} becomes concentration independent, as reported in Figure 3B. On the same figure, data[11] for $LiClO_4$ in the polyether PEO-400 (with $n = 8.0$) are reported in terms of τ_{II}^{-1} vs C_{LiClO_4}. The data seem to mesh with those of the present paper. Linear regression of all the data for concentrations up to 0.2 mol/dm^3 gives $r^2 = 0.90$, an intercept $= 2.4_8 \times 10^7$, and a slope $S = 1.9_7 \times 10^8$. Since the plateau, at high concentration, averages $\tau_{II}^{-1} = k_3 + k_3 = 6.0 \times 10^7$ s^{-1} and from the intercept $k_{-3} = 2.5 \times 10^7$ s^{-1}, it follows that $k_3 = (6.0 - 2._5) \times 10^7 = 3._5 \times 10^7$ s^{-1} and $K_3 = k_3/k_{-3} = 3.5/2.5 = 1.4$.

The finding that τ_I^{-1} and τ_{II}^{-1} are independent of chain length in the range of $n = 2$ to $n = 4.6$ for the repetition units ($-CH_2CH_2O-$) seems to indicate that the observed processes reflect the *local* relaxation dynamics of desolvation of ions with interchange of the ($-CH_2CH_2O-$) groups by $^-$NCS, *independent of the increase of chain length of the polyether*. So it appears that infrared spectra "see" the complexed species "at contact", whereas the solvent-separated species are lumped together with the hyrodynamically free species as "spectroscopically free" species.

On the other hand, ultrasonic relaxation spectra also "see" the solvent-separated species as distinguished from free ions (or hydrodynamically free ions). However, ultrasonic spectra seem to be "myopic" to the long-range interaction, with long chains attached to the reacting centers, even if these chains carry the same repetitive reacting groups such as ($-CH_2CH_2O-$) groups. These long-range interactions are reflected by the shear viscosity η of the liquids as is well known.

Table 4. Dielectric Relaxation Parameters and Solution Conductivities σ for LiSCN in 1,2-DME, Diglyme, Triglyme, and PEO-250, and PEO-400 at 25 °C

C_{LiSCN}	f_1 (GHz)	ϵ_0	$\epsilon_{\infty 1}$	f_2	$\epsilon_{\infty 2}$	σ (S cm^{-1})	β
			Solvent: 1,2-DME				
0.0867	2.1_5	8.7_0	6.9_0	42	2.7_0	$3.7_8 \times 10^{-5}$	0
0.12_7	1.8_0	9.5_3	7.1_0	39	2.7_5	7.8×10^{-5}	0
0.16_9	1.5_0	10.3_4	7.1_0	37	2.6_0	$1.3_7 \times 10^{-4}$	0
			Solvent: Diglyme				
0.050	0.90	8.35	7.70	22	2.50	$2.1_5 \times 10^{-5}$	0.14
0.10_1	0.8_0	9.4_0	7.6_5	18.8	2.50	$6.6_5 \times 10^{-5}$	0.1_4
0.15_2	0.8_6	9.7_6	7.6_5	19.3	2.50	$1.5_1 \times 10^{-4}$	0.1_1
0.20_2	0.8_0	10.5_9	7.5_4	18.8	2.50	$2.1_8 \times 10^{-4}$	0.1_4
			Solvent: Triglyme				
0.0483	0.40	8.8_0	7.7_5	16	2.7_0	$8.1_6 \times 10^{-6}$	0.1_2
			Solvent: PEO-250				
0.0494	0.2_8	8.8_5	7.9_8	9.5_0	2.6_8	$6.2_3 \times 10^{-6}$	0.1_7
0.10_0	0.2_8	9.7_3	7.9_8	9.5_0	2.6_8	1.6×10^{-5}	0.1_7
0.151	0.3_0	10.0_8	7.9_8	8.3_0	2.6_5	$2.8_7 \times 10^{-5}$	0.1_7
0.19_4	0.2_8	10.1	7.9_8	9.5_0	2.6_8	$4.5_4 \times 10^{-5}$	0.1_7
			Solvent: PEO-400				
0.10_0			8.8_5	4.3	2.5_2	$8.4_8 \times 10^{-6}$	0.3_2

The range of sensitivity of molecular interactions for the third method used in this paper, namely, UHF-microwave dielectric spectroscopy, will be considered next.

(c) Dielectric Relaxation Spectra. Figures 4A, 4B, and 4C report the ϵ_d'' and ϵ' *vs* f and Cole−Cole plots of the quantity ϵ_d'' *vs* ϵ', where ϵ_d'' is the loss coefficient (part of the complex permittivity $\epsilon^* = \epsilon' - J\epsilon''$) corrected by the conductance contribution $\epsilon_\sigma'' = 1.8 \times 10^{12}\sigma/f$. In the above, then, $\epsilon_d'' = \epsilon'' - \epsilon_\sigma''$, and ϵ' is the real component of ϵ^*. The systems reported in Figures 4A, 4B, and 4D are LiSCN at $c \approx 0.1$ mol dm^{-3} in the solvents 1,2-DME, diglyme, and PEO-250, respectively. Figure 4C reports LiSCN at $c \approx 0.05$ mol dm^{-3}, because of its limited solubility in triglyme.

The ϵ_d'' and ϵ' *vs* f and Cole−Cole plots can be described for each function ϵ' and/or ϵ_d'' by the sum of one Debye relaxation process (for the solute):

$$\epsilon' = (\epsilon_0 - \epsilon_{\infty 1})\frac{1}{1 + (f/f_1)^2}$$

$$\epsilon_d'' = (\epsilon_0 - \epsilon_{\infty 1})\frac{f/f_1}{1 + (f/f_1)^2} \qquad (6)$$

and by a Cole−Cole process for the solvent[12]

$$\epsilon' = (\epsilon_{\infty 1} - \epsilon_{\infty 2})\frac{1 + (f/f_{II})^{1-\beta}\sin(\beta\pi/2)}{1 + 2(f/f_{II})^{1-\beta}\sin(\beta\pi/2) + (f/f_{II})^{2(1-\beta)}} + \epsilon_{\infty 2}$$

$$\epsilon'' = (\epsilon_{\infty 1} - \epsilon_{\infty 2})\frac{(f/f_{II})^{1-\beta}\cos(\beta\pi/2)}{1 + 2(f/f_{II})^{1-\beta}\sin(\beta\pi/2) + (f/f_{II})^{2(1-\beta)}} \qquad (7)$$

For one of the solvents (1,2-DME), the distribution parameters $\beta = 0$ and functions (7) reduce themselves to a simple Debye process, valid at least in the frequency range investigated.[13]

Table 4 reports the parameters ϵ_0, $\epsilon_{\infty 1}$, f_1, $\epsilon_{\infty 2}$, f_2, β, where applicable, and σ, the specific conductivity (S cm^{-1}) for the systems and the concentrations investigated at 25 °C. Also the following correlations appear to be relevant to the present project:

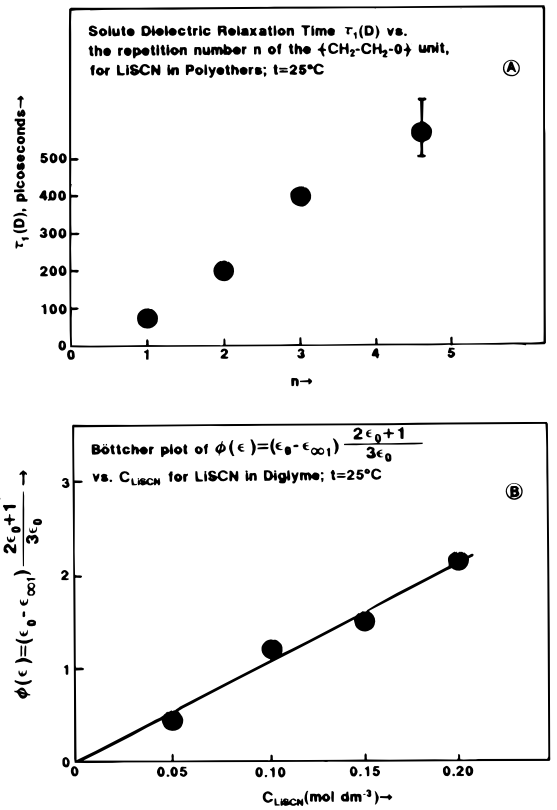

Figure 5. (A) Dielectric relaxation time for the solute $\tau_1(D)$ *vs* the repeat unit number n of the group $(-CH_2CH_2O-)$ for LiSCN in the solvents 1,2-DME, diglyme, triglyme, and PEO-250 at 25 °C. (B) Böttcher plot of the quantity $\phi(\epsilon) = (\epsilon_0 - \epsilon_\infty)(2\epsilon_0 + 1)/3\epsilon_0$ *vs* the concentration of LiSCN for the solutions in diglyme at 25 °C.

1. If one calculates the decay time of the polarization of the solution due to the solute, τ_1 $(=2\pi f_1)$, and identifies it with the rotational relaxation time of the solute $\tau_1(D)$ (assuming $\tau_1 \approx \tau_1(D)$), one may plot τ_1 *vs* the repetition number n of the $(-CH_2CH_2O-)$ group as shown in Figure 5A. With the points available, a correlation between $\tau_1(D)$ and n is discernible. If $\tau_1(D)$ reflects the rotational relaxation time due to LiNCS ion pairs, the correlation seems to suggest that $\tau_1(D)$ depends on the chain length of the solvent polyether. In other words, *the dielectric rotational relaxation time is dependent on the long-range molecular dynamics of the solvent, at variance with the conclusion reached above, for both ultrasonic and infrared spectrometries.*

2. Figure 5B reports the quantity $\phi(\epsilon) = (\epsilon_0 - \epsilon_{\infty 1})$-$(2\epsilon_0 + 1)/3\epsilon_0$ for the representative system LiSCN in diglyme plotted *vs* C_{LiSCN} according to the Böttcher function:[14]

$$\epsilon_0 - \epsilon_{\infty 1} = \frac{4\pi L C_{LiSCN}}{(1 - \alpha_d F)^2}\frac{3\epsilon_0}{2\epsilon_0 + 1}\frac{\mu^2}{3kT} \qquad (8)$$

having neglected the polarizability α_d and the reaction field factor F product, $\alpha_d F$, with respect to one. In eq 8, L is Avogadro's number and μ is the apparent dipole moment of the LiNCS ion pair.

The solid line in Figure 5B, calculated by linear regression, giving 50% statistical weight to the origin, yields a determination coefficient $r^2 = 0.99$, an intercept $I = 0.015$, and a slope $S = 10.40_{51}$, from which one calculates the apparent dipole moment $\mu = 13.0 \times 10^{-18}$

esu cm. By taking a two rigid sphere model for the dipole, $\mu = ea_\mu$, with e the electron charge and a_μ the separation distance between the two charges in the dipole, it follows that $a_\mu = 2.7 \times 10^{-8}$ cm, a reasonable parameter expressing the separation of charges in the (Li^+ $^-$NCS) dipole. The same plot for LiSCN in 1,2-DME (not shown), using the data of Table 4, giving 50% statistical weight to the origin, yields $r^2 = 0.998$, $I = 0.012$, and $S = 13.4_9$, from which $\mu = 14.8 \times 10^{-18}$ esu cm, and taking $\mu = ea_\mu$, $a_\mu = 3.1 \times 10^{-8}$ cm.

In eq 8, it has been assumed that the bulk concentration of LiSCN is approximated to that of the dipole ion pairs, a reasonable posture, in view of the conclusions drawn from the infrared spectra above. It is noteworthy, however, that if a Böttcher plot of $\Phi(\epsilon)$ *vs* C_{LiSCN} is attempted for LiSCN in PEO-250, the plot shows nonlinearity at concentrations above 0.1 mol dm^{-3}, a sign of formation of nonpolar aggregates (antiparallel dimers) at the highest concentrations in PEO-250, a phenomenon already recorded in the past.[7,16]

Conclusions

By increasing the chain length of the polymer solvent, namely, the repetition number n, infrared spectra and, eventually, ultrasonic spectra, through τ_{II}, become independent of the chain length of the polymer, at least in the range investigated of $n = 2$ to $n = 8$. This indicates that to differing extents, both methods report a *local* situation and dynamics at a small-molecule level. Dielectric relaxation, by recording the rotational dynamics of ion pairs, seems to be sensitive to the long-range molecular interaction expressed by the polymer chain length (at least up to $n = 4.6$). This may be due to the solvent chain rearrangements required for the inversion in position of cation and anion during the rotation of the dipoles, a net translational motion (per each rotation) of the partners of the dipoles.

It is hoped that the information contained in this paper will be useful in devising models for future transport theories of ions dissolved in polyethers of increasing chain length.

Acknowledgment. The authors are grateful to the Army Research Office (ARO), Durham, NC, for support through Grant DAA H04-93-G0014. R.K. is also grateful to the National Science Foundation for an undergraduate educational research grant through Polytechnic University.

References and Notes

(1) Jagodzinski, P.; Petrucci, S. *J. Phys. Chem.* **1974**, *78*, 917. Farber, H.; Petrucci, S. *J. Phys. Chem.* **1975**, *79*, 1221. Onishi, S.; Farber, H.; Petrucci, S. *J. Phys. Chem.* **1980**, *84*, 2922. Delsignore, M.; Maaser, H. E.; Petrucci, S. *J. Phys. Chem.* **1984**, *88*, 2405. Maaser, H. E.; Delsignore, M.; Newstein, M.; Petrucci, S. *J. Phys. Chem.* **1984**, *88*, 5100.

(2) Firman, P.; Xu, M.; Eyring, E. M.; Petrucci, S. *J. Phys. Chem.* **1993**, *97*, 3606.

(3) Fuoss, R. M.; Accascina, F. *Electrolytic Conductance*; Interscience: New York, 1959. Fuoss, R. M.; Hsia, K. L. *Proc. Natl. Acad. Sci. U.S.A.* **1966**, *57*, 1550.

(4) Turq, P.; Blum, L.; Bernard, O.; Kunz, W. *J. Phys. Chem.* **1995**, *99*, 822 and previous literature cited therein.

(5) Ratner, M. A. In *Polymer Electrolyte Reviews*; McCallum, J. R., Vincent, C. A., Eds.; Elsevier: London, 1987; Vol. 1.

(6) Cohen, M. H.; Turnbull, D. J. *J. Chem. Phys.* **1959**, *31*, 1164. Adams, G.; Gibbs, J. H. *J. Chem. Phys.* **1965**, *43*, 139.

(7) Maaser, H. E.; Xu, M.; Hemmes, P.; Petrucci, S. *J. Phys. Chem.* **1987**, *91*, 3047 and previous literature cited therein.

(8) Paoli, D.; Luçon, M.; Chabanel, M. *Spectrochim. Acta, Part A* **1978**, *34*, 1087. Menard, C. Doctoral Thesis, University of Nantes, France, 1973. Chabanel, M.; Wang, Z. *J. Phys. Chem.* **1984**, *88*, 1441.

(9) Eschmann, J.; Strasser, J.; Xu, M.; Okamoto, Y.; Eyring, E. M.; Petrucci, S. *J. Phys. Chem.* **1990**, *94*, 3908.

(10) Eigen, M.; Winkler, R. In *Neurosciences, Second Study Program*: Schmitt, F. O., Ed.; Rockefeller University Press: New York, 1970; p 685.

(11) Salomon, M.; Xu, M.; Eyring, E. M.; Petrucci, S. *J. Phys. Chem.* **1994**, *98*, 8234.

(12) Hill, N. In *Dielectric Relaxation and Molecular Behaviour*; Hill, N., Vaughan, W. A., Price, A. H., Davies, M., Eds.; Van Nostrand: London, 1969; Chapter 1.

(13) Saar, D.; Brauner, J.; Farber, H.; Petrucci, S. *Adv. Mol. Relax. Interact. Processes* **1980**, *16*, 263. See, however, ref 11 for 1,2-DME dissolved in cyclohexane.

(14) Cavell, E. A. S.; Knight, P. C.; Sheik, A. *Trans. Faraday Soc.* **1971**, *67*, 2225. Böttcher, C. J. F. *Theory of Electrical Polarization*; Elsevier: Amsterdam, 1952.

(15) Farber, H.; Petrucci, S. *J. Phys. Chem.* **1975**, *79*, 1221.

(16) Salomon, M.; Uchiyama, M.; Xu, M.; Petrucci, S. *J. Phys. Chem.* **1989**, *93*, 4374. Delsignore, M.; Farber, H.; Petrucci, S. *J. Phys. Chem.* **1985**, *89*, 4968.

MA9517916